sciendo

DOI: 10.2478/fbgp-2021-0001

3D CHEMOMETRIC MODEL SIMULATING THE *ACITHECA POLYMORPHA* FROND: IMPLICATIONS FOR RECONSTRUCTING CARBONIFEROUS FERNS (MARATTIALES, CANADA)

José A. D'Angelo[1,2,*], Erwin L. Zodrow[3] & Josef Pšenička[4]

[1] Universidad Nacional de Cuyo, FCEN, MS5502JMA, Mendoza, Argentina; joseadangelo@yahoo.com
[2] Palaeobotanical Laboratory, Cape Breton University, Sydney, Nova Scotia, B1P 6L2, Canada
[3] 503 Coxheath Road, Sydney, Nova Scotia, Canada, B1R 1S1; zzodrovii@gmail.com
[4] Center of Palaeobiodiversity, West Bohemian Museum in Pilsen, Kopeckého sady 2, 30100 Pilsen, Czech Republic; jpsenicka@zcm.cz
[*] Corresponding author e-mail joseadangelo@yahoo.com

Abstract: *Reported are results of an initial approximate imitation of a Carboniferous fern frond, i.e., marattialean Acitheca polymorpha (Schimper), Middle Pennsylvanian Sydney Coalfield, Canada. The simulation experiment is based on the analysis of 14 infrared spectra obtained by means of Fourier Transform Infrared spectroscopy from four detached fragments of sterile polymorphic penultimate-pinna compressions. The calculated relative, semi-quantitative, chemical data from the infrared spectra are the input for principal component analysis deriving a 3D (three-dimensional) chemometric model. To interpret it, the four specimens are placed in hypothetical-frond positions simulating a tripinnate frond, based on diminishing penultimate-rachial widths from 1-mm (distal) to 10-mm (proximal). Hypothetical conclusions include position-dependent chemistries, specifically that of opposing trends of aromaticity vs. aliphaticity in pinnules-rachises. This, in turn, would suggest potential for (i) fern-frond reconstruction, and (ii) for determination of a most likely frond position of fragmentary specimens by "chemical classification"; the predictive aspect. However, further experimental refinement is necessary particularly based on larger frond segments to confirm or disconfirm the overall hypothetical results.*

Keywords: Fossil fern, FTIR, chemical frond architecture, Carboniferous

INTRODUCTION

We have experimentally confirmed the hypothesis of the relationship between chemical trends and frond architecture for certain seed-fern fronds (Sydney Coalfield, Canada) notably by employing 3D chemometric models (D'Angelo *et al.* 2010, D'Angelo & Zodrow 2015, 2016, Zodrow *et al.* 2016, 2017, Zodrow & D'Angelo 2019). The models not only serve as a template for reconstructing seed-fern fronds and by the combination of frond architecture and chemistry for natural classification, but also for chemical predictors of missing frond parts (e.g., does this petiole chemically "fit" this particular frond?).

Earlier studies of functional-group contents and distributions in "pecopterids" showed potential for phytotaxonomy and separation from seed ferns (Zodrow & Mastalerz 2001), even when based on fragmentary specimens. Unlike the more complete seed-fern fronds collected *in situ*, fern fronds tend to be fragmented by coal-mining activity in the Sydney Coalfield (Figure 1). Nevertheless, we used this disadvantage as incentive to initiate, at least for Carboniferous palaeobotany, fern-frond simulation, i.e., *Acitheca polymorpha* (Brongniart) Schimper (Zodrow *et al.* 2006), based on chemistry. The paper is thus a logical extension of modeling foliage-venation morphology of a tripinnate-fern frond by analysis of variance and the F-test (Zodrow & Banerjee 1993) and Heggie's & Zodrow (1994) mathematical simulation experiment of also a fern frond.

In this paper, we discuss implications/statistical results of the simulation experiment, *albeit* hypothetically, to infer a relationship between chemical trends and frond architecture in *A. polymorpha*. Although known already in a general context, we

furthermore confirm the thin nature of a fern compression requiring a more "delicate" maceration procedure than the sturdier seed-fern compression for successful cuticular retrieval. Emphasized is that fern and seed-fern compressions share a common thermal history of 0.65% vitrinite reflectance of the Lloyd Cove Seam, in the Sydney Coalfield (Hacquebard 1998). Inferred not only is a relatively lower diagenetic influence, but also that value is probably one of the lowest known among Carboniferous coal basins, and suitable in chemical interpretation.

MATERIALS, SAMPLE PREPARATION, AND METHODS

Materials and abbreviations

Four specimens are selected for this study, Figs. A to D on Plate I, from the 150 *A. polymorpha* specimens collected from the roof shale of the Lloyd Cove Seam (Zodrow 1982, text-fig. 3, inset). The 150 specimens are included in the 750 specimens used in the revision of *A. polymorpha* that focuses on its biology (Zodrow *et al.* 2006).

Used in the text, figure captions, and appended tables are the following abbreviations: **Pi** for pinnule, **PUr** for penultimate rachis, both only in reference to the four study specimens. Noted is that **Pi** may either be a compression (**comp**) or fossilized-cuticle (**FC**), whereas **PUr** is preserved only as **comp** (see section: ***Sample forms comp, FC of Pi and coal* (*vitrain*)** - Lloyd Cove Seam, Figure 1).

Figure A on Plate I shows two mutually, parallel penultimate-pinna fragments. The one on the left-hand side represents nearly a complete pinna. 10 mm long **Pi** at the tip rapidly developed into ultimate pinnae distally, where dextral ultimate pinnae of both tend to be comparatively longer and are attached to a thin 1-mm **PUr** close to the frond tip (Figure 2A). Rotund **Pi** in the left specimen

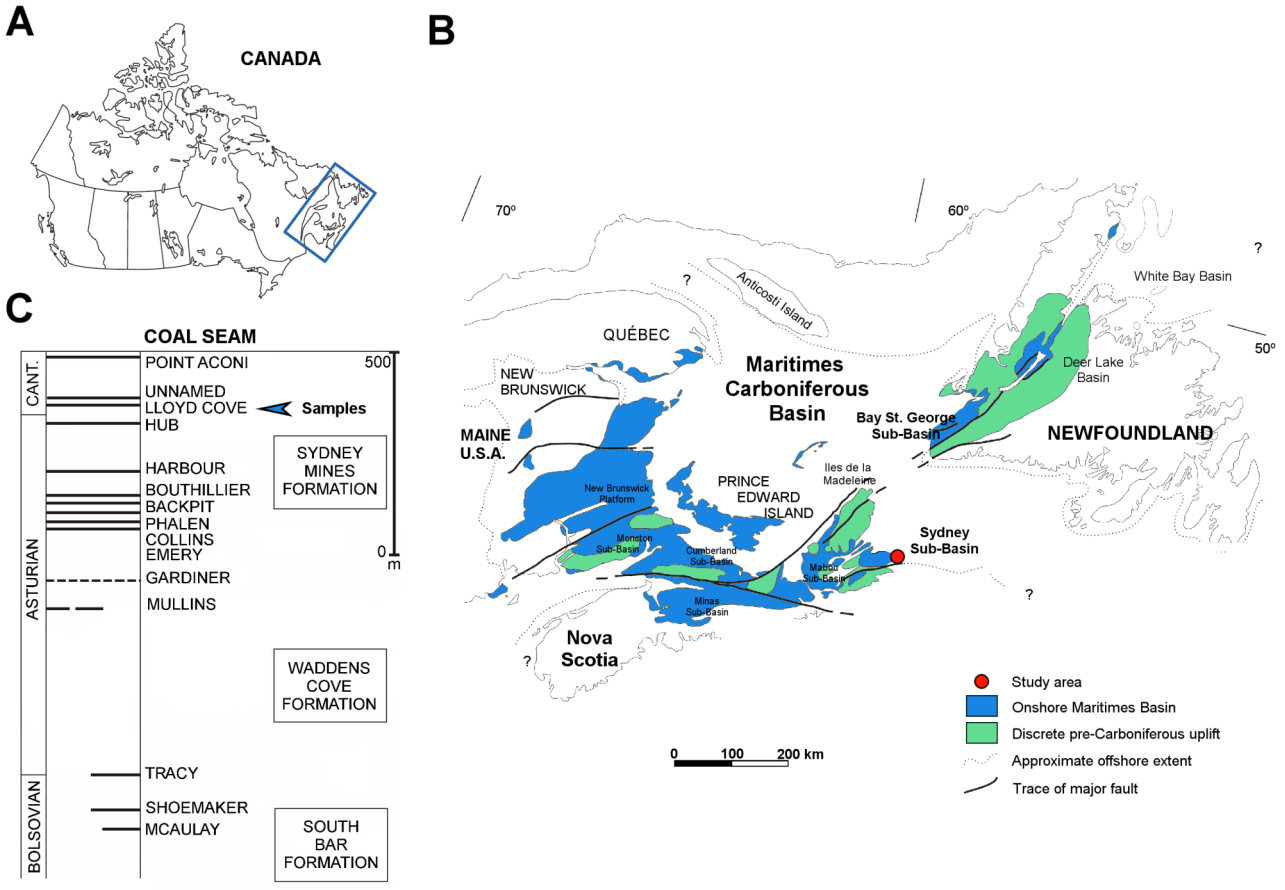

Figure 1. *Location map. A - Canada. B - Maritimes Basin with Sydney Coalfield (Sub-basin), Nova Scotia. C - Lithostratigraphic column and sample location (arrowed). CANT. = Cantabrian, currently being revised.*

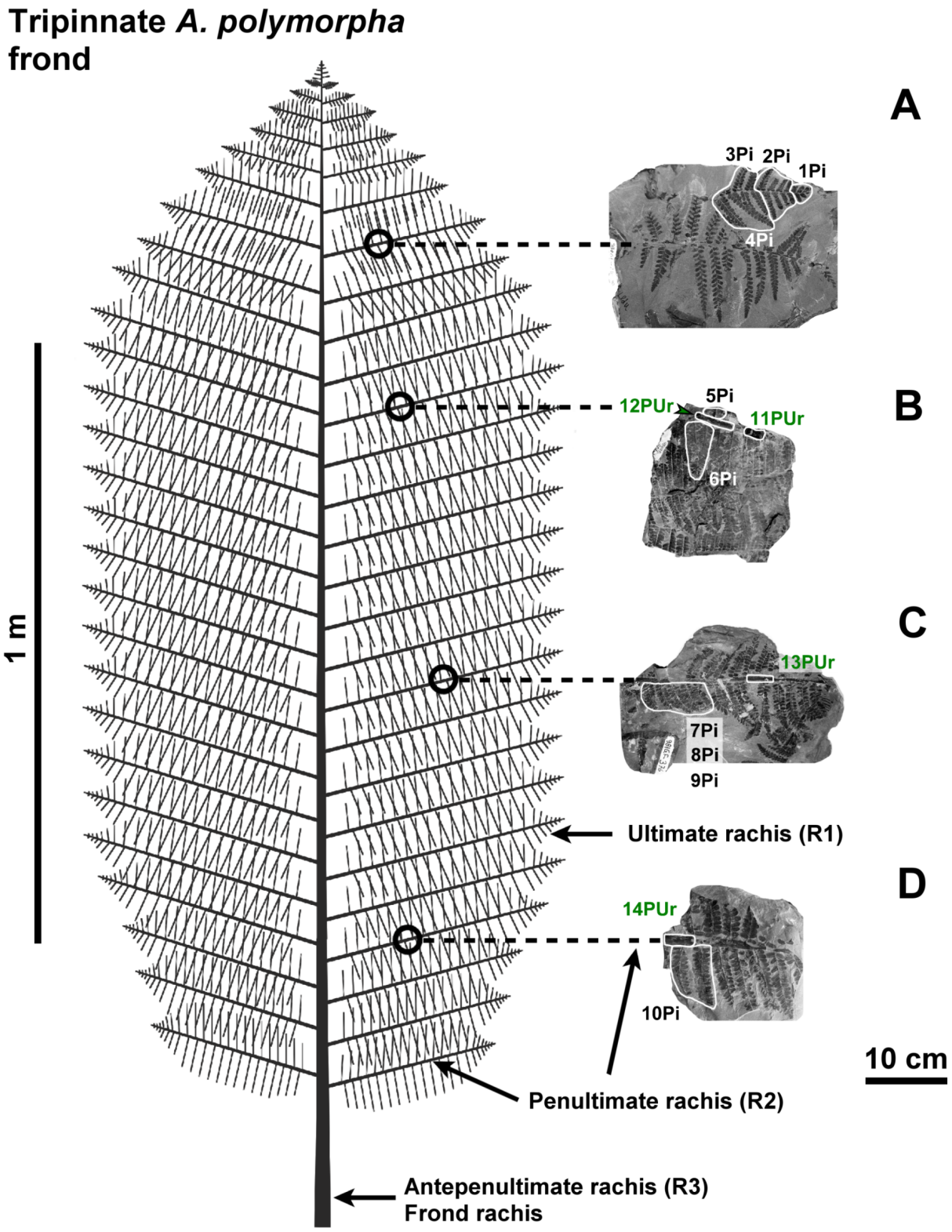

Figure 2. *Acitheca polymorpha frond and rachial designation R1, R2, and R3 according to Zodrow et al. (2006, fig. 12) showing simulated positioning of specimens in Plate I.*

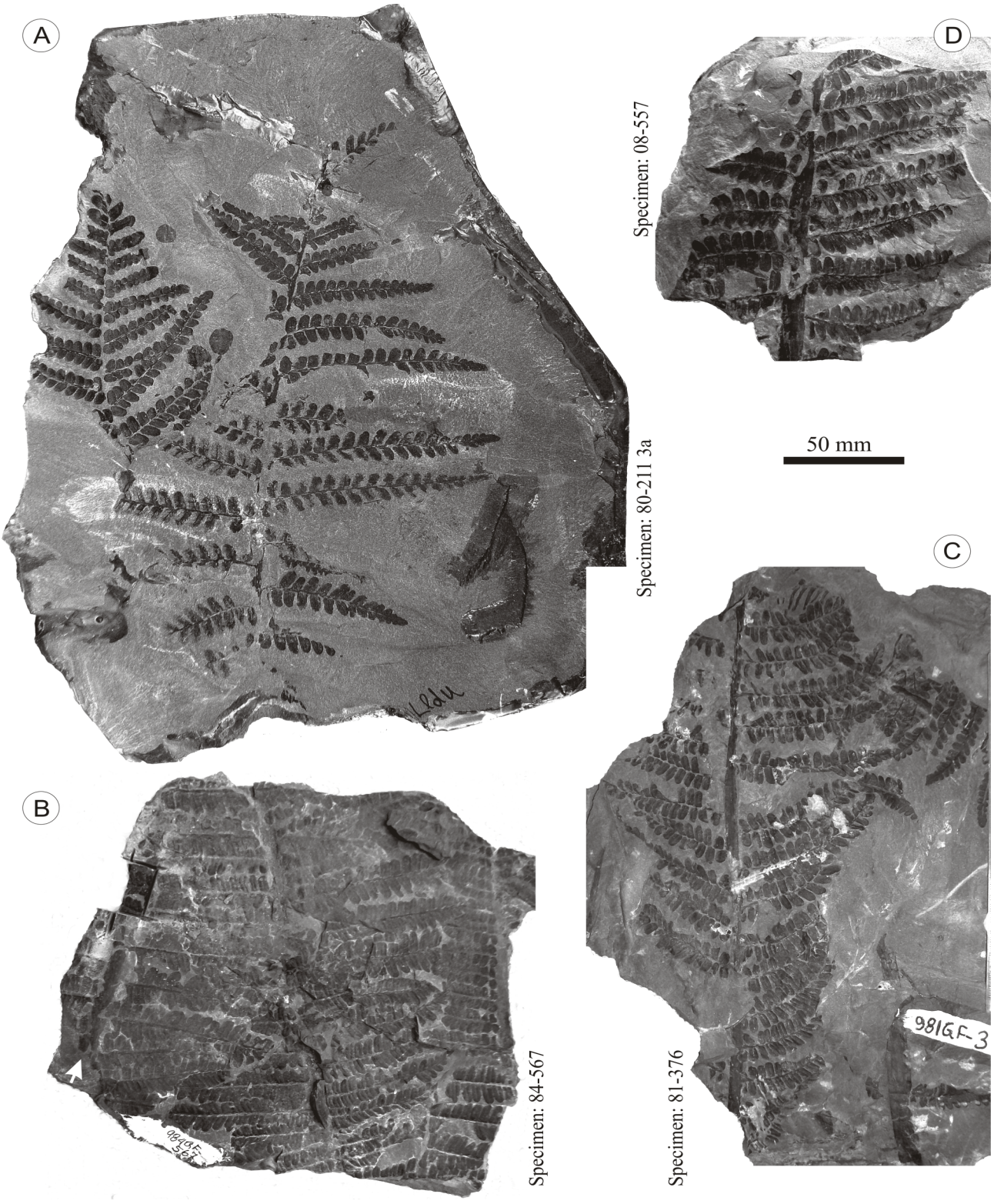

Plate I The four sterile and fragmentary *Acitheca polymorpha* specimens A to D with accession numbers constituting the sample material, Palaeobotanical Collection, Cape Breton University, Sydney, Nova Scotia, Canada. Scale bar = 5 cm applies to A, B, C, and D.

vary in length from 5 - 8 mm, are stalked and the venation in the tip **Pi** shows proximal divisions, where the top branch divides again [polymorphopterid type of venation *sensu* Cleal (2015)].

Figure B on Plate I shows three fragmentary penultimate pinnae, where the rachises are of similar 5 - 6 mm width, and entire-margined **Pi** are 9-mm long and 3 - 4 mm wide. Since they are more or less parallel and closely spaced likely indicates that they are supported by the frond rachis in the upper-middle frond part (Figure 2B).

Figure C on Plate I shows a single 300-mm long penultimate pinna whose punctate rachis decreases in width from 8 to 5 mm. **Pi** length is 10-mm with a width of 4-mm. This also represents a specimen with the longest sample **PUr** (still incomplete) among the 150 specimens mentioned earlier. Based on Fig. A on Plate I, it is clear that the frond had to be large in the order of meters, and the specimen likely originated from the middle section of the frond (see Figure 2C).

Figure D on Plate I shows a single penultimate-pinna fragment whose rachial width is 10-mm. It is not only the widest of the four study specimens but also the widest in the 150-specimen collection mentioned earlier. The **PUr** is punctate and its **Pi** are 10-mm long and 4-mm wide with slightly chordate bases. The specimen likely originated from the proximal section of the frond (see Figure 2 D).

The vitrain samples included in the analysis are from the Lloyd Cove Seam, which is underlying the shale from which the *A. polymorpha* specimens were collected.

Sample Preparation

In order to illustrate the overall morphological preservation of the studied specimens, following are some details regarding the preparation procedure for obtaining **comp** and **FC**. This includes the extraction of cuticles, which were not used either in the chemical or in the statistical analyses. In contrast with routinely liberating intact seed-fern compressions from rock matrices with 48% v/v hydrofluoric acid (HF), liberating the thin polymorphic compressions/fossilized-cuticles is tedious. They are successfully liberated intact only after using dilute 25 - 30% HF for ca. 24 h, as they completely disintegrate in 48% HF. Adhering to them are invariably thin-gelatinous films interspersed with silicate minerals and organics (Plate II, Fig. A) which after a repeated 2 to 3-time treatment with dilute HF for one hour each yielded fairly clean specimens for reliable infrared-spectra interpretation. See Fig. B on Plate II fossilized-cuticles (cf. Zodrow 1993, Zodrow & Mastalerz 2009). Equally time-consuming is cuticular extraction, as already commented on by Barthel (1962),

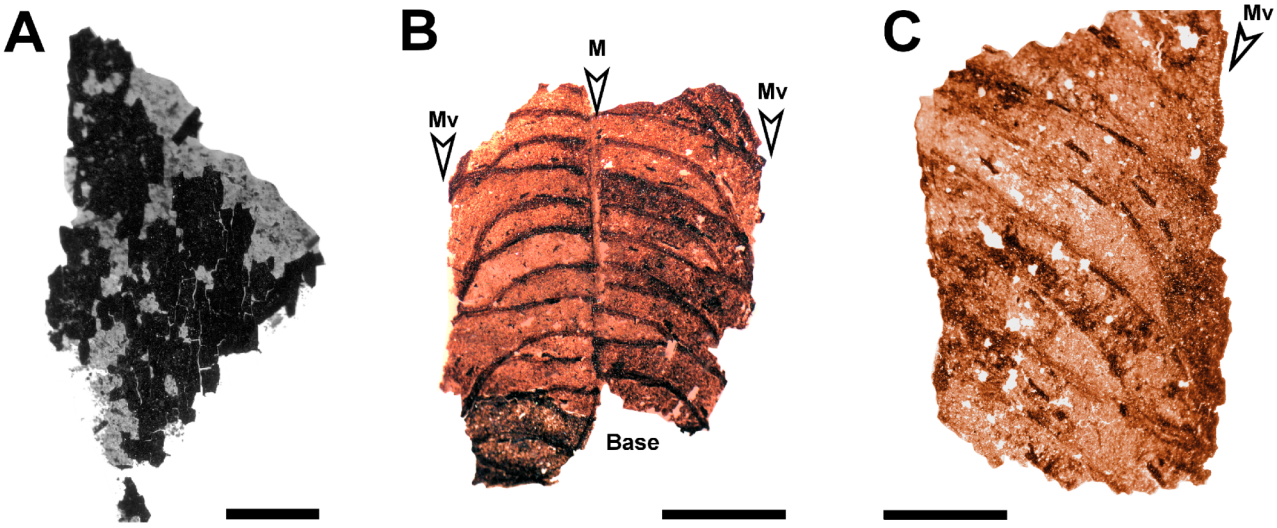

Plate II Sample forms of pinnules of *Acitheca polymorpha*. A - Non-retrievable **Pi** compression based on 48% HF treatment (Plate I, Fig. B; specimen 84-567), random location. Scale bar = 0.5 mm. B - **FC** using 25-30% HF (Plate I, Fig. D; specimen 80-557), random location. Scale bar = 1 mm. C - Cuticle using 25–30% HF (Plate I, Fig. A; specimen 80-211 3a). Scale bar = 1 mm. M = margin, and Mv = the midvein of the **Pi**.

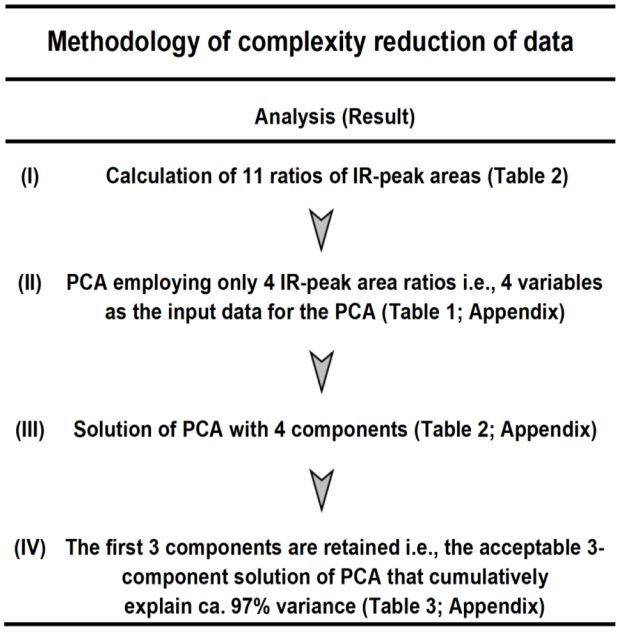

Figure 3. *Flow chart showing the methodology used for the complexity reduction of the infrared-derived data.*

Pšenička (2005), and more recently by Pšenička & Zodrow (2017). Despite trials with dilute Schulze's solutions, 25 – 30% nitric acid v/v, in combination with reduced reaction time 30 – 90 min, and 2% v/v potassium hydroxide, only millimeter-sized cuticular fragments are secured (e.g., Plate II, Fig. C).

As a consequence of the thin compressions, larger fossiliferous areas are required to supply suitable sample amounts for reliable infrared spectra (see the section *FTIR spectroscopy*). These may entail for example ca. 20 **Pi** from three adjacent ultimate pinnae, or 2 – 4 continuous cm along a **PUr** (e.g., Figure 2B). The recovered **comp** and **FC** are kept in distilled water which is repeatedly changed during 3-4 days to deacidify them to avoid as much as possible chemical interference, then they are slowly air-dried in preparation for Fourier Transform Infrared spectroscopy (FTIR) analysis.

FTIR spectroscopy

The KBr (potassium bromide)-pellet method and IR instrumentation used are those described in our previous publications for seed-fern applications which include 1.4 – 2.0 mg of compression material/spectrum, e.g., D'Angelo & Zodrow (2016). Being faced, however, with limited sample amounts as in this case of 0.1 – 1.0 mg, but striving for consistency of analytical procedure with previously published seed-fern spectra, we (i) decreased the KBr amount to 200 mg (from 250 mg), and (ii) in-

Table 1. Definition of semi-quantitative area ratios derived from FTIR spectra. See Table 2.

Area ratio # [a]	**Area-ratio name - PCA variable**	**Area ratios: Band-region (cm^{-1}) or peak position (cm^{-1})**	**Interpretation and remarks**
1	CH_2/CH_3	(~2925 + ~2850) / (~2955 + ~2870)	Methylene/methyl ratio. It relates to aliphatic chain length and degree of branching of aliphatic side groups (side chains attached to macromolecular structure; Lin & Ritz 1993a, b). Higher value implies comparatively longer and straight chains, a lower value shorter and more branched chains. Caution is advised using the ratio, as it may be misleading due to the contribution from CH_2 and CH_3 groups attached directly to aromatic rings (Petersen & Nytoft 2006).
2	CH_{al}/Ox	(3000-2800) / (1800-1600)	Aliphatic/Oxygen-containing compounds ratio. Relative contribution of aliphatic C-H stretching bands (CH_{al}) to the combined contribution of oxygen-containing groups and aromatic carbon (Ox). From higher values decreasing oxygen-containing groups can be inferred, or the lower the CH_{al}/Ox ratio, the higher the Ox term. This ratio could provide some information about oxidation in organic matter (e.g. Mastalerz & Bustin 1997, Zodrow & Mastalerz 2001).

Table 1, continued

Area ratio # [a]	Area-ratio name - PCA variable	Area ratios: Band-region (cm^{-1}) or peak position (cm^{-1})	Interpretation and remarks
3	C=O/C=C	(1700-1600) / (1600-1500)	Carbonyl/aromatic ratio of carbon groups. Relative contribution of C=O to aromatic carbon groups. Higher values indicate increasing carbonyl/carboxyl groups to aromatic carbon groups (D'Angelo 2006).
4	C=O cont	(~1714) / (1800-1600)	Carbonyl contribution. Relative contribution of carbonyl carboxyl groups (C=O; peak centered near 1714 cm^{-1}) to combined contribution of oxygen-containing groups and aromatic carbon (C=C) structures.
5	C=C cont	(~1600) / (1800-1600)	Aromatic carbon contribution. Relative contribution of aromatic carbon groups (C=C; peak in 1650 to 1520 cm^{-1} region, centered near 1600 cm^{-1}) to combined contribution of oxygen-containing groups and aromatic carbon (C=C) structures.
6	CHal/C=C	(3000-2800) / (1600-1500)	Aliphatic/aromatic carbon groups ratio. Relative contribution of aliphatic C-H stretching bands to aromatic carbon groups (C=C). Higher values indicate increasing aliphatic groups to aromatic carbon groups. This ratio is equivalent to the I1 index of Guo & Bustin (1998).
7	'A' factor = CHal/ (CHal+C=C)	(3000-2800) / [(3000-2800) + (1600-1500)]	Relative contribution of aliphatic C-H stretching bands to sum of aliphatic C-H stretching and aromatic carbon structures. According to Ganz and Kalkreuth (1987) it represents change in relative intensity of aliphatic groups.
8	'C' factor = Ox / (Ox+C=C)	(1800-1600) / [(1800-1600) + (1600-1500)]	Relative contribution of oxygen-containing compounds to the sum of oxygen-containing structures and bands of aromatic carbon. According to Ganz & Kalkreuth (1987) it represents change in carbonyl/carboxyl groups.
9	CH_{al}/C=O	(3000-2800) / (1800-1700)	Aliphatic/carbonyl groups ratio. Relative contribution of aliphatic C-H stretching bands to carbonyl/carboxyl groups (C=O). Indicator for cross-linking degree of a polymeric structure (i.e., the linking of polymer chains). Lower values indicate higher C=O content and higher cross-linking (Benítez *et al.* 2004).
10	CHar/CHal	(900-700) / (3000-2800)	Aromatic C-H out-of-plane bending/aliphatic ratio. Contribution of aromatic C-H out-of-plane bending modes to aliphatic C-H stretching bands (aliphatic H bands). Indicator for aromaticity in organic matter. Higher values indicate higher aromaticity, i.e., higher content of aromatic groups vs. aliphatic groups.
11	CH_{ar}/C=C	(900-700) / (1600-1500)	Aromatic C-H out-of-plane bending/aromatic carbon groups ratio. Ratio of integrated area of aromatic C-H out-of-plane bending deformations to those of aromatic carbon groups. Used as measure of the degree of condensation of aromatic rings.

creased the number of co-added interferograms considerably to 1,000 (from 256); where (i) and (ii) are equally applied to the pellet for the background spectrum.

The spectra are evaluated for functional-group contents and distributions in two complementary ways:

1. *Qualitative Chemical Analysis*: IR (infrared) peaks are assigned to known wavenumber absorbances of functional groups. For information applicable as well to fossil-fern analysis, readers are referred to Zodrow *et al.* (2009). Particularly focused on are functional groups that are known to be the most important in terms of general organic structures constituting compressions and fossilized-cuticles (e.g., Zodrow & Mastalerz 2001, Zodrow *et al.* 2009). Included in these groups are different types of aliphatic-, aromatic-, and oxygen-containing compounds (see the section *Semi-quantitative Analysis*).

2. *Semi-quantitative Chemical Analysis*: Eleven peak-area ratios are calculated (Tables 1 and 2) using different combinations of the four functional groups (i to iv) listed below. Peak-area ratios (fully explained referring to "1" and so forth in Table 1; see the first column: "Area ratio #") are obtained following standard methodologies, e.g., Ganz & Kalkreuth (1987), Mastalerz & Bustin (1997), Guo & Bustin (1998), Zodrow & Mastalerz (2001), D'Angelo & Zodrow (2016) and Zodrow & D'Angelo (2019).

(i) CH_2 (methylene), CH_3 (methyl), and other aliphatic (CH_{al}) groups ("1", "2", "6", "7", "9", and "10") present in aliphatic compounds;

(ii) aromatic (C=C) groups ("3", "5", "6", "7", "8", and "11") that characterize compounds containing benzene rings;

(iii) carbonyl (C=O) and other (Ox) groups ("2", "3", "4", "8", and "9"), which are found in oxygen-bearing compounds; and

(iv) aromatic (CHar) groups ("10" and "11") that are also found in benzene-ring containing compounds.

Table 2. Complete data set of semi-quantitative FTIR data (n=14) for *Acitheca polymorpha*, and FTIR data (n=3) for vitrain (V).

		1	2	3	4	5	6	7	8	9	10	11
Sample number	**Sample Form**	**CH_2/ CH_3**	**CH_{al}/ Ox**	**C=O/ C=C**	**C=O cont**	**C=C cont**	**CH_{al}/ C=C**	**'A' factor**	**'C' factor**	**CH_{al}/ C=O**	**CH_{ar}/ CH_{al}**	**CH_{ar}/ C=C**
1Pi	Comp	2.6	0.52	0.04	0.02	0.36	1.44	0.59	0.043	32.1	0.29	0.41
2Pi	Comp	2.5	0.51	0.05	0.02	0.37	1.36	0.58	0.052	25.1	0.17	0.23
3Pi	Comp	2.4	0.53	0.03	0.01	0.41	1.30	0.56	0.029	42.8	0.18	0.24
4Pi	Comp	2.4	0.34	0.03	0.01	0.36	0.93	0.48	0.028	32.4	0.08	0.07
5Pi	FC	2.1	0.38	0.08	0.03	0.40	0.97	0.49	0.072	12.5	0.20	0.19
6Pi	Comp	2.6	0.56	0.02	0.008	0.42	1.35	0.57	0.02	66.3	0.27	0.36
7Pi	Comp	1.9	0.40	0.04	0.01	0.32	1.24	0.55	0.041	28.7	0.21	0.26
8Pi	Comp	1.7	0.44	0.04	0.02	0.36	1.22	0.55	0.043	27.3	0.20	0.25
9Pi	Comp	1.6	0.48	0.04	0.02	0.36	1.33	0.57	0.042	30.3	0.23	0.30
10Pi	FC	2.3	0.46	0.08	0.02	0.29	1.58	0.61	0.074	19.7	0.13	0.20
11PUr	Comp	2.3	0.44	0.02	0.01	0.43	1.03	0.51	0.024	42.7	0.16	0.17
12PUr	Comp	1.8	0.40	0.04	0.02	0.44	0.90	0.47	0.035	25.1	0.28	0.25
13PUr	Comp	2.4	0.45	0.04	0.02	0.53	0.85	0.46	0.036	22.5	0.30	0.26
14PUr	Comp	2.3	0.43	0.04	0.01	0.39	1.10	0.52	0.036	29.9	0.26	0.29
V	Vitrain	0.9	0.54	0.003	0.002	0.77	0.69	0.41	0.0027	258.4	0.63	0.44
V	Vitrain	0.8	0.40	0.030	0.020	0.74	0.54	0.35	0.026	20.5	0.84	0.46
V	Vitrain	1.0	0.42	0.007	0.005	0.64	0.67	0.40	0.0072	92.5	0.78	0.52

Statistical methods

Principal component analysis (PCA) is a non-parametric, pattern-recognizing method frequently used at it is most basic for visualizing multivariate data in a simplified way. This is achieved through data reduction, where the number of components is less than the number of variables, and through data grouping using component scores (e.g. Jolliffe 2002, Johnson & Wichern 2008, Izenman 2008). Inherent assumptions include uncorrelated (orthogonal) components, no error variance and data structure.

PCA was performed using the computer program STATISTICA® (StatSoft Inc. 2012) on raw data consisting of four variables with 17 determinations each. Our strategy was to evolve a set of data groupings to evaluate it as a function of functional groups that represent the chemical structures.

We have demonstrated time and again that for the studied seed ferns the following four calculated peak-area IR ratios (Table 1):
(1) CH_2/CH_3;
(2) C=O/C=C;
(3) C=C cont; and
(4) 'A' factor

account for the largest relative accumulated-explained variance (information) in PCA of the chemical composition of compressions, fossilized-cuticles, and vitrain samples (D'Angelo 2006, 2019, D'Angelo & Zodrow 2015, 2020). Accordingly, in the present analysis, we retained three components whose explained cumulative variance is higher than 95% (Tables 3 – 5; see Kaiser 1960

Table 3. Input correlation matrix of four variables with unity in the principal diagonal.

	CH_2/CH_3	**C=O/C=C**	**C=C cont**	**'A' factor**
CH_2/CH_3	1	0.407652	-0.759956	0.735800
C=O/C=C	0.407652	1	-0.606851	0.471953
C=C cont	-0.759956	-0.606851	1	-0.877718
'A' factor	0.735800	0.471953	-0.877718	1

Table 4. Solution of principal component analysis (PCA).

Variable	**Component 1**	**Component 2**	**Component 3**	**Component 4**	
CH_2/CH_3	0.856583	0.313237	0.408964	0.029957	1
C=O/C=C	0.693087	-0.713400	0.087485	0.055111	1
C=C cont	-0.954967	-0.038931	0.153384	0.250989	1
'A' factor	0.914769	0.206562	-0.289111	0.192211	1
Eigenvalue	2.96287	0.65124	0.28202	0.10388	4
Cumulative explained variance %	74.0717	90.3527	97.4031	100	

Table 5. Acceptable three-component PCA solution.

Variable	**Component 1**	**Component 2**	**Component 3**	**Variance ***
CH_2/CH_3	0.856583	0.313237	0.408964	99.91
C=O/C=C	0.693087	-0.713400	0.087485	99.70
C=C cont	-0.954967	-0.038931	0.153384	93.70
'A' factor	0.914769	0.206562	-0.289111	96.31
Eigenvalue	2.96287	0.65124	0.28202	3.89613
Cumulative explained variance %	74.0717	90.3527	97.4031	

* Variance explained by first 3 PCs (%).

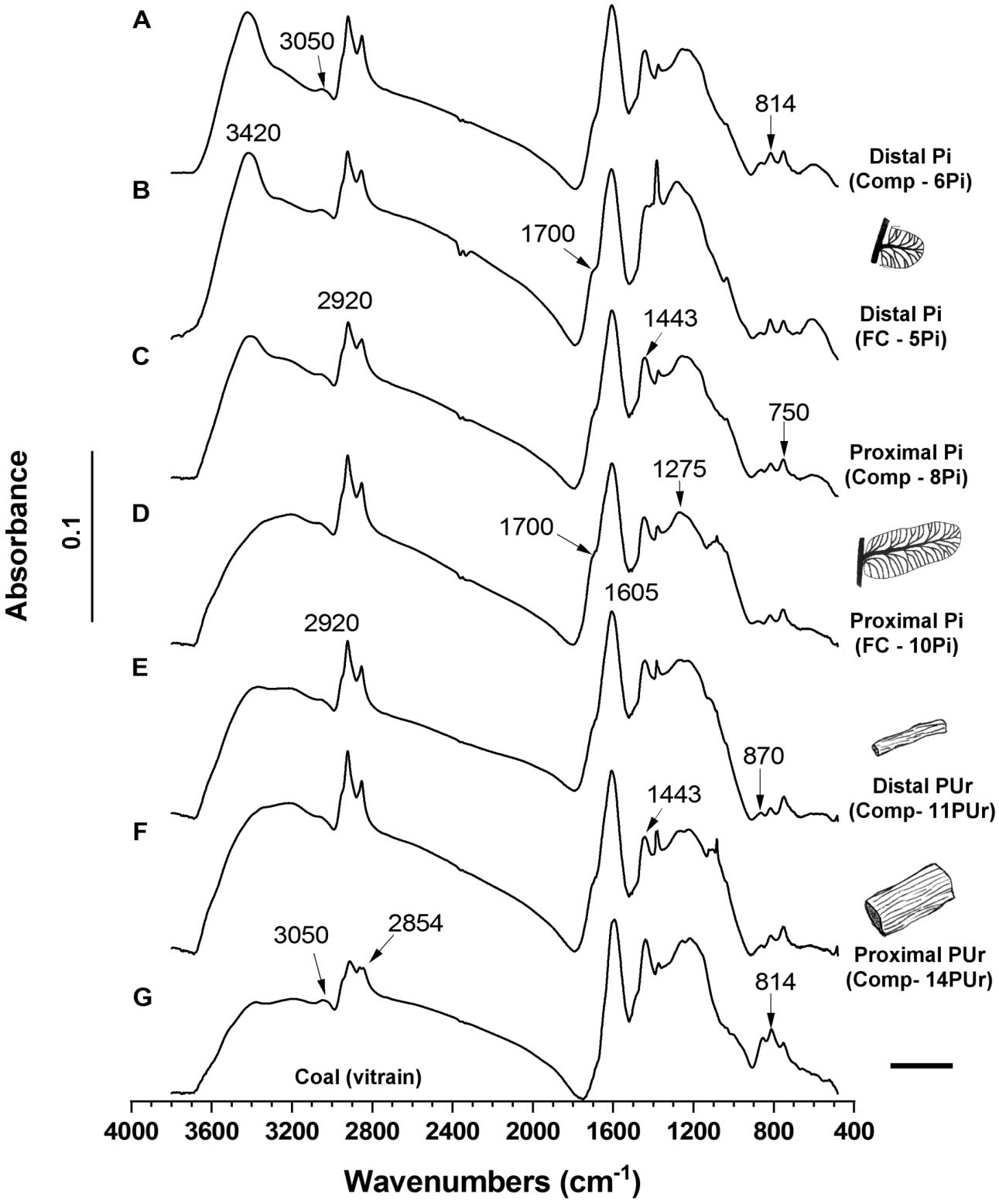

Figure 4. *Selected infrared spectra of proximal and distal **Pi** and **PUr**. Coal (vitrain; Lloyd Cove Seam) spectrum is shown for comparison. Scale bar = 5 mm. Pen sketches are to scale.*

and Kendall 1965 for other methods). Deletion of the seven calculated peak-area IR ratios from the present PCA simplifies interpretation including pictorial presentations. This procedure (Figure 3) underpins the *raison d'être* of the 3D model as a *de facto* parsimonious interpretative approach (Izenman 2008).

One-way-analysis of variance (ANOVA) is a statistical method for significant tests between means of two or more data groups (Fisher 1970, Zodrow & Banerjee 1993). Underlying assumptions include (i) normal-data distribution (although appreciable deviation from normality is not a problem because of robustness, see Donaldson 1966), (ii) homoscedasticity, and (iii) independent variables.

We considered the calculated PC 1, PC 2, and PC 3 values as proxies for the chemical composition of **Pi** and **PUr** and used ANOVA to test their similarities/differences (Tables 6 – 8). In this way, we made ANOVA comparisons considering several combinations of **Pi** and **PUr** from different frond positions (distal and proximal).

The simulated *A. polymorpha* frond

The framework for the analytical FTIR data to use 3D chemometrics for an approximate frond imitation (Lat. simulo) and testing by ANOVA assumes a tripinnate frond (Figure 2). The macromorphological criteria for the proposed positioning of the four specimens (Plate I) are the decreasing widths of their **PUr** in conjunction with the size (width) of the penultimate pinnae, the size of the ultimate pinnae, and the **Pi** venation pattern.

RESULTS

FTIR Data

Representative **Pi** and **PUr** FTIR spectra are illustrated in Figure 4. From a qualitative point-of-view, and irrespective of the sample studied, **comp** (Figure 4A, C, E, and F) and **FC** spectra (Figure 4B and D) look similar. All share certain functional groups, particularly in the aliphatic- and oxygen-containing zones.

Following are the assignations of the main IR peaks (in decreasing wavenumber magnitudes), some of which were used to calculate IR peak-area ratios (bracketed numbers refer to the list in section *FTIR spectroscopy*).

3420 cm^{-1}: O-H hydroxyl stretching;
3050 cm^{-1}: aromatic C-H stretching;
2920, 2854 cm^{-1}: aliphatic C-H stretching (i);
1700 cm^{-1}: C=O stretching (iii);
1605 cm^{-1}: aromatic C=C (ii);
1443 cm^{-1}: alkyl bending;
1275 cm^{-1}: C-O stretching;
870 cm^{-1}, 814 cm^{-1}, and 750 cm^{-1}: aromatic C-H out-of-plane bending (iv).

Hypothetical 3D Multivariate-Frond Model

Three principal components (PC) account for 97.40% cumulative variance (see Tables 3–5). Plots of component loadings and component scores are shown in Figure 5A–F.

PC 1 (74.07% explained variance) has high positive loadings on CH_2/CH_3, 'A' factor, and C=O/C=C, and a high negative loading on C=C cont (Figure 5A). This pattern probably reflects the abundance of longer and straight, aliphatic chains containing oxygen-bearing compounds vs. aromatic-carbon functionalities.

The proximal 14**PUr** as well as the distal 1**Pi**, 2**Pi**, 3**Pi**, 4**Pi**, 6**Pi**, the proximal 7**Pi**, 8**Pi**, 9**Pi**, and the two **FC** 5**Pi** and 10**Pi** (= Figure D on Plate I = Figure B on Plate II) exhibit positive scores against PC 1 (Figure 5B, x axis). This probably is linked to the medium to high contents of aliphatic compounds with longer and relatively straight hydrocarbon chains.

Vitrain samples, as well as the distal 11**PUr**, 12**PUr**, and proximal 13**PUr**, have negative scores against PC 1 (Figure 5B, C, x axis), as a probable consequence of their medium to high values of aromatic contents (Table 2).

PC 2 (16.28% explained variance) has a high negative loading on the C=O/C=C ratio reflecting the abundance of carbonyl-containing groups. This possibly includes ester bridges, which are related to the cross-linking degree of the macropolymeric structures (a cross link is a chemical bond that connects one polymeric chain to another one; Solomons *et al.* 2014). Higher values of the C=O/C=C ratio probably correlate with higher C=O contents and possibly a higher cross-linking degree (Table 2; see also Benítez *et al.* 2004). Distal compressions 1**Pi**, 2**Pi**, 3**Pi**, 4**Pi**, 6**Pi**, and distal 11**PUr** and proximal 14**PUr** have medium to low C=O/C=C values (Figure 5B, C, y axis). On the other hand, proximal **comp** 7**Pi**, 8**Pi** and 9**Pi**,

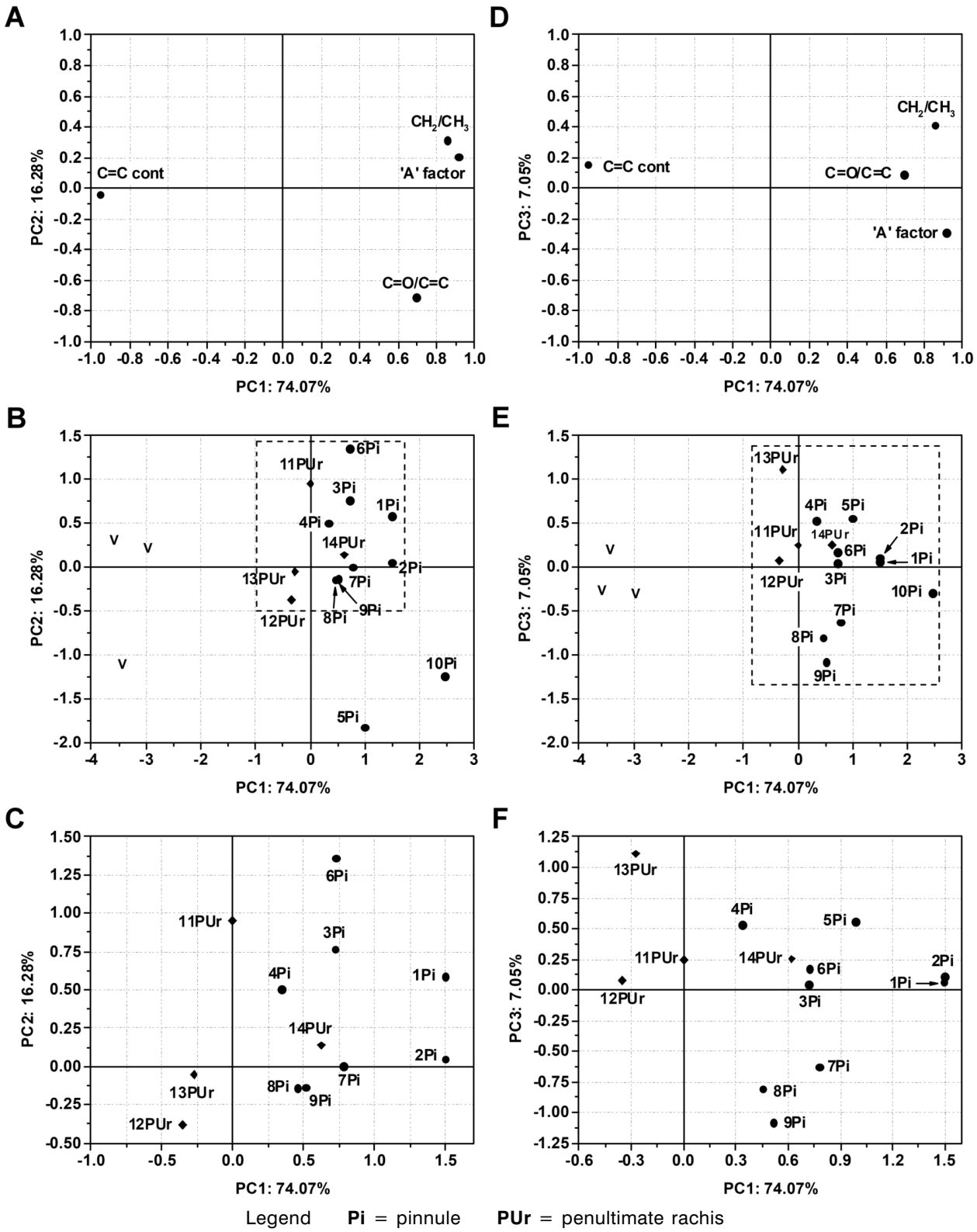

Figure 5. *Principal component analysis (PCA). A – Plot of PC 1 vs. PC 2 component loadings. B – Full-scale plot of PC 1 vs. PC 2 component scores. C – Detail of the zone delimited in B. D – Plot of PC 1 vs. PC 3 component loadings. E – Full-scale plot of PC 1 vs. PC 3 component scores. F – Detail of the zone delimited in E.*

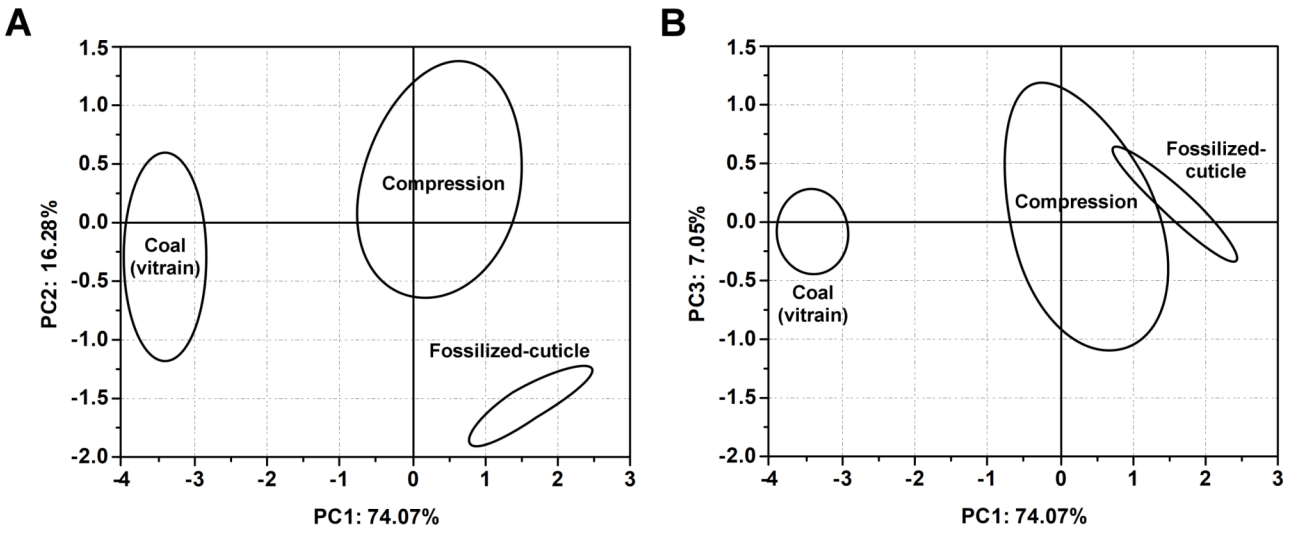

Figure 6. *Simplified plots of A – Fig. 5B and B - Fig. 5E showing groupings of data as approximately delimited by elliptical zones (with no statistical significance).*

as well as proximal 12**PUr** and distal 13**PUr** have intermediate values the of C=O/C=C ratio. The highest values of the C=O/C=C ratio recorded for **FC** (i.e., 5**Pi** and 10**Pi**) explain their high negative scores against PC 2 (Table 2).

PC 3 (7.05% explained variance) has a moderate positive loading on the CH_2/CH_3 ratio, as well as a moderate negative loading on the 'A' factor. All **PUr** and most 1**Pi**, 2**Pi**, 3**Pi**, 4**Pi**, 5**Pi**, and 6**Pi** have positive scores against PC 3 (Figure 5E, F, y axis), as a consequence of their medium to high values of CH_2/CH_3 (Table 2). Proximal 7**Pi**, 8**Pi**, 9**Pi**, and 10**Pi** have negative scores against PC 3 because of their very low values of CH_2/CH_3. These results indicate that all the penultimate rachises and the distal pinnules have comparatively longer and straighter polymethylenic chains than proximal pinnules.

Sample Forms Comp, FC of Pi, and Coal (vitrain)

Score plots (Figure 5B, C, E, and F) reflect the main chemical characteristics of the three sample forms. A simplified, full-scale plot of PC 1 vs. PC 2 component scores (see Figure 5B) is shown by Figure 6A, whereas Figure 6B represents the corresponding simplified plot of PC 1 vs. PC 3 component scores (see Figure 5E). Ellipses delimiting the forms do not have any statistical significance. This interpretation (Figure 6A: PC 1 vs. PC 2) underscores and parallels the distinct statistical separation of these sample forms demonstrated for seed ferns by Zodrow & Mastalerz (2001, 2009) and Zodrow *et al.* (2009).

Simplified plots of component scores (PC 1 vs. PC 2 and PC 1 vs. PC 3; Figure 6A, B, respectively) are useful in showing the data grouping as dependent on chemical functionalities.

The group representing vitrain is chemically very different, as indicated by the values of C=C cont (aromatics), which are the highest of the entire sample set (Table 2).

Evident is that the **FC** are derived from **comp**. This possibly took place through complex processes of preservation controlled by still only partly known physicogeochemical factors (e.g., Zodrow & Mastalerz 2009, Lafuente Diaz *et al.* 2018, D'Angelo & Zodrow 2020).

Chemometrics and Architecture of *A. Polymorpha*, The 3D PCA Model

The utility of the chemometric approach for analyzing the discrimination of structural groups and the hypothetical relationship between frond architecture and semi-quantitative chemistry is addressed in this section.

Figure 7A, B and Figure 7C, D are simplified plots of Figure 5B, C and Figure 5E, F, respectively. PC 1 vs. PC 2 (Figure 7A) and PC 1 vs. PC 3 (Figure 7C) plots show two groups representing **Pi** and **PUr** (for clarity, coal and FC are not shown).

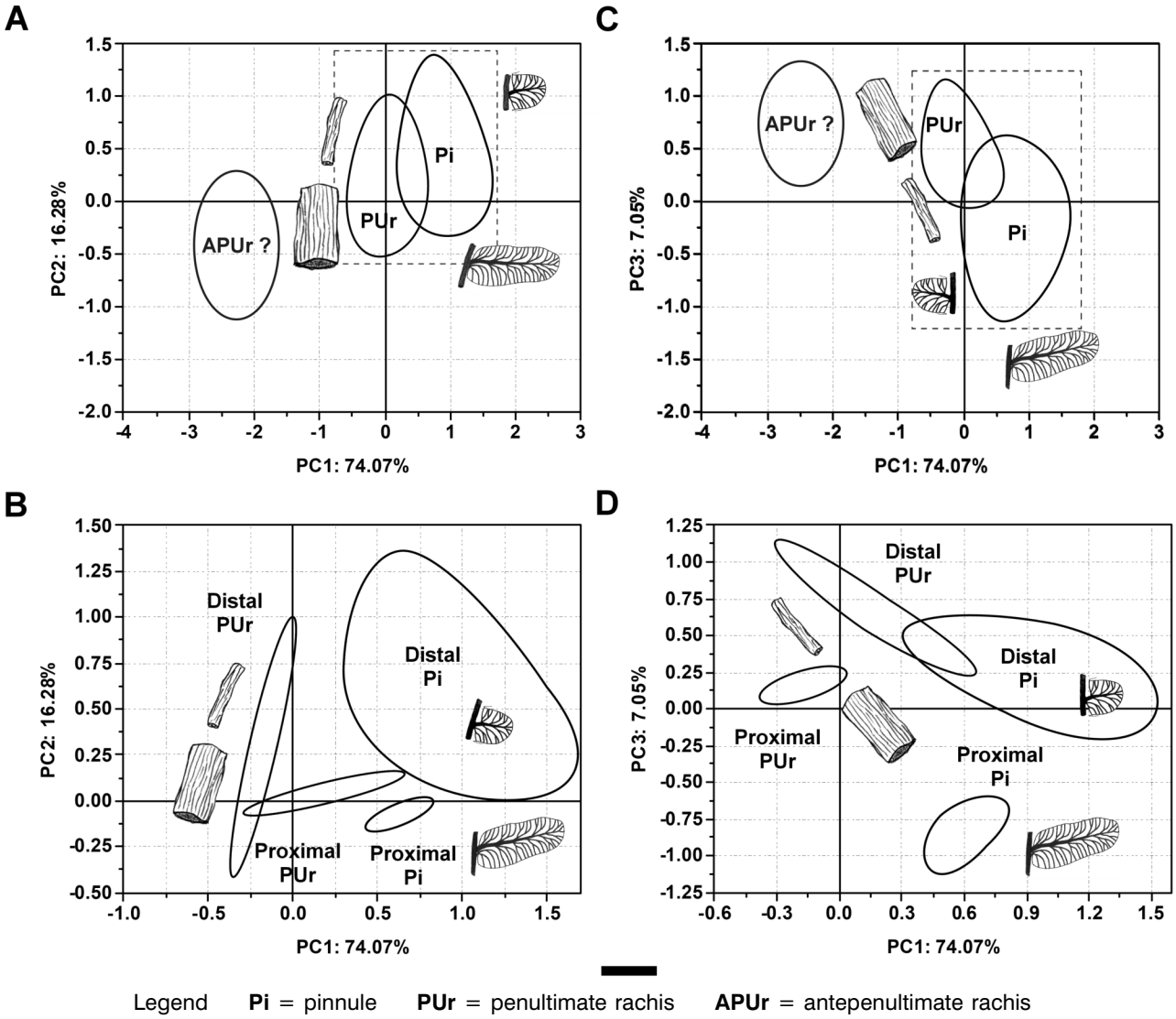

Figure 7. *Simplified plots of Fig. 5B, C, E, and F. A – Full plot (PC 1 vs. PC 2) indicating data groupings for different frond parts i.e.,* ***Pi*** *and* ***PUr****. B – Detail of the area delimited in A showing approximate zones corresponding to proximal and distal locations of* ***Pi*** *and* ***PUr****. C – Full plot (PC 1 vs. PC 3). D – Detail of the area delimited in C. Encircled '****APUr****' represents the zone corresponding to a predicted chemical composition of an antepenultimate rachis. Elliptical zones are for clarity only. Scale bar = 5 mm. Pen sketches are to scale. For simplicity, coal (vitrain) and* ***FC*** *are not shown.*

Overall, the 3D PCA model shows that all specimens have somewhat different contents of aliphatic-, aromatic-, and oxygen-containing functionalities. However, the two groups of **Pi** and **PUr** overlap (Figure 7A, B), which indicates that basically some parts of the frond share some functional groups.

The insufficiently recovered sample amounts of the ultimate rachises preclude their FTIR analysis. Nevertheless, morphological characteristics provide insights into their likely chemical composition (see the exhaustive revision of *Acitheca* Schimper by Zodrow *et al.* 2006). Ultimate and penultimate rachises of the *A. polymorpha* frond (Zodrow *et al.* 2006) are punctate, longitudinally striate, possibly representing cortical, sclerenchymatous fibers. Some rachises show metaxylemic tracheids with simple, scalariform wall thickenings and pitting (see Zodrow *et al.* 2006, pl. III, fig. 7 and pl. V, figs 5, 6). These morphological charac-

teristics suggest that the chemical composition of pinnules could have been very similar to their corresponding ultimate rachises, and the nearby penultimate rachises. It is well-known that in living plants sclerified tissues, e.g., xylem and hypodermis, because of their high-aromatic composition are among the plant structures with the highest fossil-preservation potential (van Bergen *et al.*, 1995, Boyce *et al.*, 2003, de Leeuw *et al.* 2006). This is the case of the sclerified tissues present in the once-living *A. polymorpha* plant. Overall, the 3D model shows that **Pi** have relatively higher aliphatic contents with longer polymethylenic side chains and lower amounts of aromatics than **PUr**. The decreasing order of aromaticity from **PUr** to **Pi** is interpreted to reflect the decreasing order of preserved, aromatic-rich compounds derived from lignin and other polyphenols.

Although the internal anatomy is not preserved, it could reasonably be assumed that the anatomical features of *A. polymorpha* could have been similar to those reported for the few known, anatomically-preserved (permineralized) specimens of other marattialean foliage. This is the case of the limonitized pinnules assigned to *Acitheca adaensis* (Marattiales; Middle Pennsylvanian, Oklahoma, U.S.A.; Mapes & Schabilion 1979, p. 692). These authors indicate that *"… A single vascular strand enters the pinnule base and extends as a prominent midrib to near the apex…"* In these pinnules, a prominent sclerotic hypodermis is usually filled with dark shiny contents. The presence of such sclerified or lignified structures suggests an aromatic-rich composition for *A. adaensis* pinnules.

Because of the morphological and anatomical continuities among tissues, and the simple, one-strand vascularization of pinnules, very similar structural-chemical compositions could be expected for the midribs and the ultimate (and possibly penultimate) rachises of *A. adaensis*. Argued is

Table 6. Results of one-way ANOVA ($\alpha = 0.05$). Comparisons amongst values of PC 1, PC 2, and PC 3 of pinnule (**Pi**) and penultimate rachis (**PUr**) samples of *Acitheca polymorpha*.

Variable (explained variance)	Frond part	*N*	Mean	SD	*F*	*P*	Decision Rule[a]	Interpretation
PC 1 (74.07%)								
	Pi **PUr**	8 4	0.81433 -0.00148	0.44579 0.44224	8.97337	0.01345	SD	**Pi** have significantly higher contents of long and straight aliphatic chains with oxygen-containing compounds than **PUr**. The latter are significantly more aromatic than the former.
PC 2 (16.28%)								
	Pi **PUr**	8 4	0.3751 0.16499	0.52795 0.56688	0.40382	0.53939	NSD	The C=O contents, and possibly the cross-linking degree of **Pi** and **PUr** are not significantly different.
PC 3 (7.05%)								
	Pi **PUr**	8 4	-0.19824 0.42202	0.56509 0.46632	3.55275	0.08881	NSD	**Pi** and **PUr** do not differ significantly in C=O contents.

[a] Null hypothesis: The means of all selected datasets are equal. At the 0.05 level, the population means could be significantly different (SD; if $p < 0.05$) or not significantly different (NSD; if $p > 0.05$).

Table 7. Results of one-way ANOVA (α = 0.05). Comparisons amongst values of PC 1, PC 2, and PC 3 of **Pi** and **PUr** of *Acitheca polymorpha* from proximal and distal frond positions.

Variable (explained variance)	Frond part / Position in frond[a]	*N*	Mean	SD	*F*	*P*	Decision Rule[b]	Interpretation
	Pi							
PC 1 (73.97%)	Distal	5	0.95363	0.5179	1.37081	0.28606	NSD	Statistically, distal and proximal **Pi** have very similar contents of aliphatic chains (with similar length and branching degree) and aromatic compounds.
	Proximal	3	0.58217	0.1725				
PC 2 (16.28%)	Distal	5	0.65402	0.47443	6.81118	0.04013	SD	Distal **Pi** have significantly lower C=O contents (and cross-linking degree) than proximal pinnules.
	Proximal	3	-0.08977	0.08203				
PC 3 (7.05%)	Distal	5	0.18604	0.20115	44.34791	0.00055	SD	
	Proximal	3	-0.8387	0.22862				
	PUr							
PC 1 (74.07%)	Distal	2	-0.17607	0.24865	0.52463	0.54414	NSD	Statistically, distal and proximal **PUr** have very similar contents of aliphatic chains (with similar length and branching degree) and aromatic compounds. Distal and proximal **PUr** have very similar C=O contents (and cross-linking degree).
	Proximal	2	0.17311	0.63481				
PC 2 (16.28%)	Distal	2	0.28729	0.94133	0.13232	0.75089	NSD	
	Proximal	2	0.0427	0.13464				
PC 3 (7.05%)	Distal	2	0.1622	0.12079	1.41248	0.35664	NSD	
	Proximal	2	0.68184	0.60642				

[a] Arbitrary classification of frond parts.
Distal **Pi**: 1**Pi**, 2**Pi**, 3**Pi**, 4**Pi**, 5**Pi**, 6**Pi**; Proximal **Pi**: 7**Pi**, 8**Pi**, 9**Pi**, 10**Pi**
Distal **PUr**: 11**PUr**, 12**PUr**; Proximal **PUr**: 13**PUr**, 14**PUr.**

[b] Null hypothesis: The means of all selected datasets are equal. At the 0.05 level, the population means could be significantly different (SD; if $p < 0.05$) or not significantly different (NSD; if $p > 0.05$).

that this is very likely the case for the four specimens of *A. polymorpha*, which in turn, could explain the chemical similarities between **PUr** and **Pi**, i.e., overlapping functional groups in the 3D PCA model. The trend in the distribution/relative concentration of aromatic compounds found is: pinnules < penultimate rachis; **Pi** < **PUr**.

However, it could reasonably be speculated that (i) ultimate rachises are chemically indistinguishable from **Pi**, and (ii) antepenultimate rachises of a tripinnate frond could have occupied the "empty zone" existing between the groups that represent **PUr** and vitrain in the 3D component space (Figure 5B and E; see also Figure 7A, C). If so, and considering the possibly more vitrainized composition of antepenultimate rachises, the likely order of aromaticity expected for *A. polymorpha* should be: pinnules (≈ ultimate rachis?) < penultimate rachis (< antepenultimate rachis?). **Pi** (≈ ultimate rachis?) < **PUr** (< antepenultimate rachis?).

Table 8. Results of one-way ANOVA (α = 0.05). Comparisons amongst values of PC 1, PC 2, and PC 3 of pinnule (**Pi**) and penultimate rachis (**PUr**) samples of *Acitheca polymorpha*.

Variable (explained variance)	Position in frond / Frond part[a]	*N*	Mean	SD	*F*	*P*	Decision Rule[b]	Interpretation
	Distal							
PC 1 (74.07%)	**Pi**	5	0.95363	0.5179	8.03363	0.03649	SD	Distal **Pi** have significantly higher contents of long and straight aliphatic chains than distal **PUr**.
	PUr	2	-0.17607	0.24865				
PC 2 (16.28%)	**Pi**	5	0.65402	0.47443	0.53777	0.49628	NSD	The latter are significantly more aromatic than the former.
	PUr	2	0.28729	0.94133				
PC 3 (7.05%)	**Pi**	5	0.18604	0.20115	0.02301	0.88537	NSD	The C=O contents, and ossibly the cross-linking degree of distal **Pi** and distal **PUr** are not significantly different.
	PUr	2	0.1622	0.12079				
	Proximal							
PC 1 (74.07%)	**Pi**	3	0.58217	0.1725	1.30248	0.33661	NSD	Statistically, proximal **Pi** and proximal **PUr** have very similar contents of both aliphatic chains (with similar length and branching degree) and aromatic compounds.
	PUr	2	0.17311	0.63481				
PC 2 (16.28%)	**Pi**	3	-0.08977	0.08203	2.00022	0.25219	NSD	The C=O contents, and possibly the cross-linking degree, of proximal **Pi** and proximal **PUr** are similar.
	PUr	2	0.0427	0.13464				
PC 3 (7.05%)	**Pi**	3	-0.8387	0.22862	17.62362	0.02466	SD	
	PUr	2	0.68184	0.60642				

[a] Arbitrary classification of frond parts.

Distal **Pi**: 1**Pi**, 2**Pi**, 3**Pi**, 4**Pi**, 5**Pi**, 6**Pi**; Proximal **Pi**: 7**Pi**, 8**Pi**, 9**Pi**, 10**Pi**

Distal **PUr**: 11**PUr**, 12**PUr**; Proximal **PUr**: 13**PUr**, 14**PUr**.

[b] Null hypothesis: The means of all selected datasets are equal. At the 0.05 level, the population means could be significantly different (SD; if $p < 0.05$) or not significantly different (NSD; if $p > 0.05$).

Chemical Differences Among Pi and PUr

IR spectra show that structural/chemical groups in these two entities are nevertheless similar, but not the same. However, our chemometric model emphasizes the relatively different contents and distributions of aliphatic, aromatic, and oxygen-containing compounds. The distal part includes 1**Pi**, 2**Pi**, 3**Pi**, 4**Pi**, 5**Pi**, 6**Pi**, 11**PUr**, and 12**PUr**, whereas the proximal one includes 7**Pi**, 8**Pi**, 9**Pi**, 10**Pi**, 13**PUr**, and 14**PUr**.

PC 1, PC 2, and PC 3 data are considered proxies for the chemical composition of pinnules and penultimate rachises, and illustrated are some test results using ANOVA, as follows:

(a) Proximal + distal Pi vs. proximal + distal PUr:

With 95% confidence (α = 0.05), significant mean differences are revealed ($p < 0.05$; Table 6) among **Pi** and **PUr** samples. In fact, **Pi** have a relative higher amounts of aliphatics with straight and

longer polymethylenic side chains (higher values of 'A' factor and CH_2/CH_3) than **PUr**. On the other hand, the latter have relatively higher contents of aromatics (higher values of C=C cont) than **Pi**. The carbonyls contents (C=O/C=C values) and, possibly, the cross-linking degree of **Pi** and **PUr** are not significantly different.

(b) Proximal vs. distal Pi:
Revealed are similar, relative contents of aliphatic chains (having similar length and branching degrees = similar CH_2/CH_3 values) as well as aromatic compounds (similar values of C=C cont). However, distal **Pi** have significantly lower C=O contents (and cross-linking degree) than proximal ones (Table 7).

(c) Proximal vs. distal PUr:
Despite the limited sample number of only four specimens (Plate I), the 3D model illustrates their chemical characteristics (cf. Table 7), and underlines similar relative contents of aliphatic chains (with similar length and branching degree), carbonyls, and aromatic compounds.

(d) Proximal Pi vs proximal PUr:
A more detailed analysis of the relative basal part of the simulated frond indicates that proximal **PUr** and their **Pi** do not chemically differ significantly (Table 8). Both have very similar contents of aliphatic chains with similar length and branching degree, as well as aromatic compounds, and possibly carbonyls contents.

(e) Distal Pi vs. distal PUr:
Finally, a more detailed analysis indicates that distal **Pi** have significantly higher contents of aliphatics with long and straight chains than distal **PUr**, whereas the latter are significantly more aromatic than the former (Table 8). The carbonyls contents, and possibly the cross-linking degree of distal **Pi** and distal **PUr** are not significantly different.

Summarizing (**a**) to (**e**):

(i) The hypothetical trends in functional-group distributions include the higher aliphatic character of **Pi** and the higher aromaticity of **PUr**.

(ii) From proximal to distal parts, and considering all the **Pi** only, a relatively homogeneous distribution of aliphatic and aromatic compounds is shown, although their carbonyl contents decrease toward the distal parts.

(iii) From proximal to distal parts, and considering all the **PUr** only, a relatively homogeneous distribution of all the studied functional groups is inferred.

(iv) Considering only the proximal **Pi** + **PUr**, the distribution of functional groups is relatively homogeneous.

(v) Considering only the distal **Pi** + **PUr** the distribution of functional groups is somewhat heterogeneous, i.e., the biggest differences among them are recorded.

(vi) We can say with 95% confidence that based on decreasing/increasing widths of the penultimate rachises, the specimen sequence in (Figure 2) reflects agreement between the simulated frond and the chemical data.

A Chemical Comparison with an Extant Pinnate-Fern Foliage

To the best of our knowledge, there are no other IR-based multivariate models including pinnules and their corresponding rachises from Paleozoic ferns, which precludes comparisons with our *A. polymorpha* 3D chemometric model.

Published, however, are FTIR data from the extant tropical, eusporangiate tree-fern *Cyathea caracasana* (Cyatheaceae; Zodrow & Mastalerz 2010) that demonstrate some common chemical groups in the ultimate rachises and the pinnule laminae. An explanation would entail similarities in tissue compositions as a result of their morphological and anatomical continuities from the penultimate/ultimate rachises to the pinnules. An example is the distinct infrared band at 1634 cm^{-1} (see Zodrow & Mastalerz 2010, fig 2C and D) which is assigned to carbonyls in the highly conjugated ketonic structures present in lignins of sclerified structures. This could be the case of tissues for the vascular strands in ultimate rachises of *C. caracasana*, which enter the pinnule bases and extend as a midrib.

Similar to the hypothetical trends shown by our 3D model for *A. polymorpha*, the *C. caracasana* FTIR data indicate chemical differences between distal (apical) and proximal (basal) pinnules (see Zodrow & Mastalerz 2010, fig 2A and C).

CONCLUSION

It is axiomatic that the spectral data derived from the four fragmentary, sterile specimens (Plate I) are valuable in themselves, signaling the first attempt of applying systematic-infrared (FTIR) analysis to Carboniferous-fern fronds. This includes the testable hypothesis of delicate and thin compressions/cuticles/fossilized-cuticles being due to the relative lower contents of aromatic (benzene-related) compounds linked to oxygen-containing molecular groups. This would imply lower contents of aromatic ether and ester bridges in the chemical structure of cutin-like macropolymers constituting the cuticles and other foliar structures/tissues. In contrast, medullosalean pinnules have higher contents of structurally more complex aromatics linked to oxygen-bearing functional groups and thicker compressions/cuticles as a consequence, noting exceptions. Moreover, in each of the four specimens, pinnules are the more aliphatic and penultimate rachises the more aromatic entities, which is accentuated in the distal sample relative to the proximal one. In the pinnules, the contents of carbonyls and other oxygen-containing compounds decrease toward the tip of the bipinnate structure. Chemical differences between proximal and distal pinnules shown by the 3D PCA model mimic those recorded for the extant fern *C. caracasana*. However, trends of aromaticity vs. aliphaticity are not sufficiently known and caution is advised when using this trend as a taxonomic parameter to differentiate among fossil-fern taxa.

The most promising insights gained from this simulative experiment are summarized as follows: (1) The 3D PCA model reflects the tripinnate nature of the *A. polymorpha* frond, combined with (2) the hypothesis of a chemistry-architecture relationship. This in turn, encourages future research on basic structural-frond relationships between seed fern and fern, notwithstanding the obvious differences in their pinnate complexity.

ACKNOWLEDGEMENTS

Noted is that the late Prof. C.A. Arnold (Michigan State University) in 1976-77, Profs. H.W. Pfefferkorn (University of Pennsylvania, USA) in 1980, and R.H. Gastaldo (Colby College, USA) in 1981 sorted out the ca. 150 specimens of *Pecopteris polymorpha* Brongniart from among many other pecopterids in the Sydney Coalfield without dissent. These then were later incorporated in the 750 specimens used in the revision of *Acitheca polymorpha*. Generous funds for these undertakings were thankfully provided to E. L. Zodrow by the University College of Cape Breton, under the academic and research leadership of the late Father Prof. D.F. Campbell, Principal (1970-1983). Our thanks go to Prof. K. Jones and Senior Lab Instructor J. MacInnis (Biology and Chemistry Departments, respectively, Cape Breton University, Sydney, Nova Scotia, Canada), for the uses of research microscopes and the FTIR instrument.

We are greatly indebted and grateful to C.J. Cleal (Cardiff), and an anonymous journal reviewer for thoughtfully focused comments and suggestions to improve the technical part and style. This contribution was partly supported by the Research Program of the West Bohemian Museum in Pilsen (DKRVOZCM2020-25/91P).

REFERENCES

Barthel, M. 1962. Epidermisuntersuchungen an einigen inkohlten Pteridospermenblättern des Oberkarbons und Perms. *Geologie, Beiheft 33*, 1-140.

Benítez, J. & Matas, A. J., Heredia, A. 2004. Molecular characterization of the plant biopolymer cutin by AFM and spectroscopic techniques. *Journal of Structural Biology 147*, 179–184.

van Bergen, P.F., Collinson, M.E., Scott, A.C. & de Leeuw, J.W. 1995. Unusual resin chemistry from Upper Carboniferous pteridosperm resin rodlets, 149–169. In Anderson, K.B., Crelling, J.C. (eds) *Amber, Resinite and Fossil Resins Symposium Series 617*. American Chemical Society, Washington, D.C.

Boyce, C.K., Cody, G.D., Fogel, M.L., Hazen, R.M., Alexander, C.M.O.'D. & Knoll, A.H. 2003. Chemical evidence for cell wall lignification and the evolution of tracheids in early Devonian plants. *International Journal of Plant Sciences 164*, 691–702.

Cleal, C.J. 2015. The generic taxonomy of Pennsylvanian age marattialean fern frond adpressions. *Palaeontographica Abt. B 292*, 1-21.

D'Angelo, J.A. 2006. Analysis by Fourier transform infrared spectroscopy of *Johnstonia* (Coryps-

tospermales, Corystospermaceae) cuticles and compressions from the Triassic of Cacheuta, Mendoza, Argentina. *Ameghiniana 43*, 669-685.

D'Angelo, J.A. 2019. Molecular structure of the cuticles of *Dicroidium* and *Johnstonia* (Corystospermaceae, Triassic, Argentina). Ecophysiological adaptations of two chemically indistinguishable, morphology-based taxa. *Review of Palaeobotany and Palynology 268C*, 109-124.

D'Angelo, J.A. & Zodrow, E.L. 2015. Chemometric study of structural groups in medullosalean foliage (Carboniferous, fossil Lagerstätte, Canada): Chemotaxonomic implications. *International Journal of Coal Geology 138*, 42-54.

D'Angelo, J.A. & Zodrow, E.L. 2016. 3D chemical map and a theoretical life model for *Neuropteris ovata* var. *simonii* (index fossil, Asturian, Late Pennsylvanian, Canada). *International Journal of Coal Geology 153*, 12-27.

D'Angelo, J.A. & Zodrow, E.L. 2020. Preservation of *Neuropteris ovata* in roof shale and in fluvial crevasse-splay facies (Late Pennsylvanian, Sydney Coalfield, Canada). Part I: An infrared-based chemometric model. *Palaios 35*, 94-109.

D'Angelo, J.A., Zodrow, E.L. & Camargo, A. 2010. Chemometric study of functional groups in Pennsylvanian gymnosperm plant organs (Sydney Coalfield): Implications for chemotaxonomy and kerogen formation. *Organic Geochemistry 41*, 1312-1325.

de Leeuw, J.W., Versteegh, G.J.M. & van Bergen, P.F. 2006. Biomacromolecules of algae and plants and their fossil analogs. *Plant Ecology 182*, 209–233.

Donaldson, T.S. 1966. Power of the F-test for non-normal distributions and unequal error variances. *United States Air Force Project RAND*. Memorandum RM-5072-PR.

Fisher, R.A. 1970. *Statistical Methods for Research Workers*. 362 pp. Oliver & Boyd, Edinburgh, London.

Ganz, H. & Kalkreuth, W. 1987. Application of infrared spectroscopy to the classification of kerogen types and the evolution of source rock and oil shale potential. F*uel 66*, 708-711.

Guo, Y., Bustin & R.M. 1998. Micro-FTIR spectroscopy of liptinite macerals in coal. *International Journal of Coal Geology 36*, 259-275.

Hacquebard, P.A. 1998. *Petrographic, physic-chemical, and coal facies studies of ten major seams of the Sydney Coalfield, of Nova Scotia*. Geological Survey of Canada Bulletin 520, 1-46.

Heggie, M. & Zodrow, E.L. 1994. Fractal lobatopterid frond (Upper Carboniferous marattialean tree fern). *Palaeontographica Abteilung B 232*, 35-57. Invited Festschrift: Prof. Dr. Hans-Joachim Schweitzer, Editor.

Izenman, A.J. 2008. *Modern Multivariate Statistical Techniques: Regression, Classification, and Manifold Learning*. 734 pp. Springer (Springer Texts in Statistics), New York.

Johnson, R.A. & Wichern, D.W. 2008. *Applied Multivariate Statistical Analysis*. 761 pp. Pearson Education Limited, New Jersey.

Jolliffe, I.T. 2002. *Principal Component Analysis*. 487 pp. Springer, New York.

Kaiser, H.F. 1960. The application of electronic computers to factor analysis. *Educational and Psychological Measurement 20*, 141–151.

Kendall, M.G. 1965. *A Course in Multivariate Analysis*. 185 pp. Charles Griffin & C. Ltd., London.

Lafuente Diaz, M.A., D'Angelo, J.A., Del Fueyo, G.M. & Zodrow, E.L. 2018. Fossilization model for *Squamastrobus tigrensis* foliage in the volcanic-ash deposit: Implications for preservation and taphonomy (Podocarpaceae, Lower Cretaceous, Argentina. *Palaios 33*, 323-337.

Lin, R. & Ritz, G.P. 1993a. Reflectance FT-IR microspectroscopy of fossil algae contained in organic-rich shale. *Applied Spectroscopy 47*, 265–271.

Lin, R. & Ritz, G.P. 1993b. Studying individual macerals using i.r. microspectroscopy, and implications on oil versus gas/condensate proneness and "low-rank" generation. *Organic Geochemistry 20*, 695–706.

Mapes, G. & Schabilion, J.T. 1979. A new species of *Acitheca* (Marattiales) from the Middle Pennsylvanian of Oklahoma. *Paleontology 53*, 685-694.

Mastalerz, M. & Bustin, R.M. 1997. Variation in chemistry of macerals in coals of the Mist Mountain Formation, Elk Valley coalfield, British Columbia, Canada. *International Journal of Coal Geology 33*, 43-59.

Petersen, H.I. & Nytoft, H.P. 2006. Oil generation capacity of coals as a function of coal age and aliphatic structure. *Organic Geochemistry 37*, 558–583.

Pšenička, J. 2005. *Taxonomy of Pennsylvanian-Permian ferns from coal basins in the Czech Republic and Canada*. 185 pp. PhD thesis, Faculty of Science, Charles University, Czech Republic.

Pšenička, J. & Zodrow, E.L. 2017. Cuticles from Pennsylvanian marattialean fern *"Pecopteris" polypodioides* (C. Presl in Sternberg) Němejc from Pilsen Basin (Czech Republic) and Sydney Coalfield (Canada). *Folia Musei Rerum Naturalium Bohemiae Occidentalis , Geologica et Paleobiologica 51(1-2)*, 13-22.

Solomons, T.W.G., Fryhle, C.B. & Snyder, S.A. 2014. *Organic Chemistry*. 1248 pp. John Wiley & Sons, Inc., New York.

STATSOFT INC. 2012. *Statistica—data analysis software system*, version 11. New York.

Zodrow, E.L. 1982. Recent palaeobotanical studies, Sydney Coalfield, Cape Breton Island, Nova Scotia, Canada, 193-198. *In* Mamet, B.L. & Copeland, M.J. (eds), Third North American Paleontological Convention, Montreal, PQ.

Zodrow, E.L. 1993. On cuticular preservation (Carboniferous medullosan, marattialean and pecopterid foliage) Sydney Coal Field, Nova Scotia, Canada. *Comptes Rendus, Douziéme* Congrès International de la Stratigraphie et Géology du Carbonifere et Permien, Buenos Aires, septembre 22-27, 1991, 2, 155-158.

Zodrow, E.L. & Banerjee, S.K. 1993. Modeling the lobatopterid frond (tree fern, Carboniferous). *Comptes Rendus, Douziéme* Congrès International de la Stratigraphie et Géology du Carbonifere et Permien, Buenos Aires, septembre 22-27, 1991, 1, 159-172.

Zodrow, E.L. & D'Angelo, J.A. 2019. Chemometric-based, 3D chemical-architectural model of *Odontopteris cantabrica* Wagner (Medullosales, Pennsylvanian, Canada): *Implications for natural classification and taxonomy. International Journal of Coal Geology 207*, 12-25.

Zodrow, E.L. & Mastalerz, M. 2001. Chemotaxonomy for naturally macerated tree-fern cuticles (Medullosales and Marattiales), Carboniferous Sydney and Mabou Sub-Basins, Nova Scotia, Canada). *International Journal of Coal Geology 47*, 255-275.

Zodrow, E.L. & Mastalerz, M. 2009. A proposed origin for fossilized Pennsylvanian plant cuticles by pyrite oxidation (Sydney Coalfield, Nova Scotia, Canada). *Bulletin of Geosciences 84*, 227-240.

Zodrow, E.L. & Mastalerz, M. 2010. Reconstruction of light environment for Pennsylvanian marattialean ferns: Insights from FTIR analysis of living *Cyathea caracasana*. *Bulletin of Geosciences 85*, 361-365.

Zodrow, E.L., Šimůnek, Z., Cleal, C.J., Bek, J. & Pšenička, J. 2006. Taxonomic revision of the Palaeozoic marattialean fern *Acitheca* Schimper. *Review of Palaeobotany and Palynology 138*, 239-280.

Zodrow, E.L., D'Angelo, J.A., Mastalerz, M. & Keefe, D. 2009. Compression-cuticle relationship of seeds ferns: Insights from liquid-solid states FTIR (Late Palaeozoic-Early Mesozoic, Canada-Spain-Argentina). *International Journal of Coal Geology 79*, 61-73.

Zodrow, E.L., D'Angelo, J.A. & Cleal, C.J. 2016. The *Neuropteris ovata* frond and its cyclopteroids: micromorphology-spectrochemistry-fractal taxonomy: Propositions for restructuring and taxonomy (Pennsylvanian, Canada). *Bulletin of Geosciences 91*, 669-704.

Zodrow, E.L., D'Angelo, J.A. & Cleal, C.J. 2017. 3D chemometric model and frond architecture of *Alethopteris ambigua* (Medullosales): Implications for reconstruction and taxonomy. *Palaeontographica Abteilung B 295*, 91-133.